ATLAS NOTE

ATLAS-CONF-2013-001

21 December 2012
Minor revision: 5 January 2013

Search for direct stop production in events with missing transverse momentum and two b-jets using 12.8 fb^{-1} of pp collisions at $\sqrt{s} = 8$ TeV with the ATLAS detector

The ATLAS Collaboration

Abstract

The results of the search for direct pair production of bottom squarks are reinterpreted in terms of direct pair production of top squarks decaying exclusively into a bottom quark and a chargino. The dataset used corresponds to an integrated luminosity of 12.8 fb^{-1} of pp collisions at $\sqrt{s} = 8$ TeV recorded by the ATLAS detector at the LHC. Assuming that the mass difference between the chargino and the lightest neutralino is small ($\lesssim 5$ GeV), top squarks with masses < 580 GeV are excluded at 95% confidence level for $m_{\tilde{\chi}_1^0} \simeq 100$ GeV and neutralino masses up to 300 GeV are excluded for $m_{\tilde{t}_1} \simeq 500$ GeV. In the case of larger mass differences ($\lesssim 20$ GeV) the top squark and neutralino mass limits weaken by up to 100 GeV.

Note number revised on 5 January 2013

ATLAS-CONF-2013-001
07/01/2013

1 Introduction

Supersymmetry (SUSY) [1–9] provides a solution to the hierarchy problem of the Standard Model (SM) by introducing supersymmetric partners of the known bosons and fermions [10–13]. In *R*-parity conserving SUSY scenarios SUSY particles are produced in pairs at the LHC. Each SUSY particle subsequently decays (possibly via intermediate SUSY particles) to Standard Model particles and a lightest supersymmetric particle (LSP), which is stable. This generically results in collider signatures with relatively large missing transverse momentum.

Naturalness arguments [14–16] require the masses of the superpartners closely connected to the Higgs sector to be near the electroweak scale. In particular, the lightest of the third generation squarks (the stop and sbottom), the fermionic partners of the Higgs bosons (the higgsinos), and to a lesser extent, the partner of the gluon (the gluino) are required to be relatively light. The other SUSY particles, on the other hand, are not constrained by naturalness criteria, and may have masses much larger than 1 TeV.

A search for pair production of the lightest sbottom particle ($\tilde{b}_1$), each decaying into a bottom quark (b) and a neutralino ($\tilde{\chi}_1^0$) has been recently performed in ATLAS [17]. Pair produced stops ($\tilde{t}_1$) may mimic this signature if they decay into a b-quark and a chargino ($\tilde{\chi}_1^\pm$), and the mass difference between the chargino and the neutralino is small. This possibility is a general feature of scenarios where the LSP is mainly higgsino or wino, and the other gauginos are much heavier.

In this note, the search for the pair production of bottom squarks presented in Ref. [17] is reinterpreted in terms of stop pair production. A simplified scenario is considered, in which the stop decays exclusively via $\tilde{t}_1 \to b\tilde{\chi}_1^+$, and $\tilde{\chi}_1^+$ decays via $\tilde{\chi}_1^+ \to W^*\tilde{\chi}_1^0 \to \tilde{\chi}_1^0 f\bar{f}'$, with f and f' representing different fermion types according to the SM branching ratios of the W boson. In case of small values for $\Delta m \equiv m_{\tilde{\chi}_1^+} - m_{\tilde{\chi}_1^0}$, f and f' are soft and may have transverse momenta below the reconstruction thresholds applied in the analysis. This leads to the final state signature of two b-tagged jets and $E_{\mathrm{T}}^{\mathrm{miss}}$ for which the sbottom pair production was designed. Two different values of Δm are considered: 5 GeV and 20 GeV. In addition, a few models with $\Delta m = 10$ GeV are considered to evaluate the analysis efficiency in an intermediate scenario. In this study, only models that are not excluded by the LEP lower limit on the chargino mass of 103.5 GeV [18] are considered.

In Section 2, differences in selection efficiency between top squark pair events and bottom squark pair events are discussed. The results are presented in Section 3, and conclusions are given in Section 4.

2 Comparison with the search for sbottom pair events

Since differences between stop and sbottom production cross sections are negligible [19], the main difference between the analysis sensitivities is the eventual change in acceptances. A summary of the different signal regions considered in the analysis of Ref. [17] can be found in Table 1. The sensitivity of this analysis (optimised for sbottom pair production) to stop pair production depends strongly on Δm. For a small mass splitting, the signal acceptance is expected to be similar to the equivalent sbottom pair produced events (with $m_{\tilde{b}_1} = m_{\tilde{t}_1}$ and same $m_{\tilde{\chi}_1^0}$). The situation gradually changes with larger mass splitting due to the presence of additional SM particles in the stop decay chains. This is expected to reduce the efficiency of some of the selections used in the signal region definitions, namely the lepton veto, the third jet veto used in signal region 1 (SR1), and $H_{\mathrm{T},n} < 50$ GeV used in SR2 and SR3.

Description	Signal region			
	SR1	SR2	SR3a	SR3b
Trigger	$E_{\mathrm{T}}^{\mathrm{miss}}$ trigger $>99\%$ efficient for $E_{\mathrm{T}}^{\mathrm{miss}} > 150$ GeV			
Event cleaning	Common to all SR			
Lepton veto	No e/μ with $p_{\mathrm{T}} > 10$ GeV			
$E_{\mathrm{T}}^{\mathrm{miss}}$	> 150 GeV	> 200 GeV	> 150 GeV	> 250 GeV
Leading jet $p_{\mathrm{T}}(j_1)$	> 130 GeV, $\lvert\eta\rvert < 2.8$	> 60 GeV, $\lvert\eta\rvert < 2.8$	> 130 GeV, $\lvert\eta\rvert < 2.8$	> 150 GeV, $\lvert\eta\rvert < 2.8$
Second jet $p_{\mathrm{T}}(j_2)$	> 50 GeV, $\lvert\eta\rvert < 2.8$	> 60 GeV, $\lvert\eta\rvert < 2.8$	> 30 GeV, < 110 GeV, $\lvert\eta\rvert < 2.8$	
Third jet $p_{\mathrm{T}}(j_3)$	veto event if $p_{\mathrm{T}}(j_3) > 50$ GeV, $\lvert\eta\rvert < 2.8$		> 30 GeV, $\lvert\eta\rvert < 2.8$	
$\Delta\phi(E_{\mathrm{T}}^{\mathrm{miss}}, j_1)$	-		> 2.5	
jet b-tagging ($\lvert\eta\rvert < 2.5$)	j_1 and j_2 tagged		j_1 anti-tagged, j_2 and j_3 tagged	
$\Delta\phi_{\mathrm{min}}(n)$	> 0.4 ($n = 2$)		> 0.4 ($n = 3$)	
$E_{\mathrm{T}}^{\mathrm{miss}}/\mathrm{m}_{\mathrm{eff}}(j_1, j_2, j_3)$	> 0.25			
m_{CT}	$> 150, 200, 250, 300$ GeV	> 100 GeV	-	
$H_{\mathrm{T},x}$	-	< 50 GeV, $x = 2$	< 50 GeV, $x = 3$	

Table 1: Summary of the event selection in each signal region. The leading, subleading and 3rd leading jet are referred to as j_1, j_2 and j_3, respectively.

Table 2 compares the SR1 selection efficiencies for sbottom pair production and stop pair production models with $m_{\tilde{b}_1,\tilde{t}_1} = 500$ GeV, $m_{\tilde{\chi}_1^0} = 300$ GeV, and $\Delta m = 5$ GeV, 10 GeV and 20 GeV. For stop pair production, the fraction of events passing the lepton veto decreases with increasing Δm, due to the presence of additional leptons passing the object identification criteria. The remaining selection steps, including the veto on the third jet, have similar efficiencies for all the samples considered.

The distributions of the third hardest jet and the number of leptons are shown in Figure 1, comparing the models considered in Table 2. Figure 2 shows the distributions of the $H_{\mathrm{T},n}$ variables used in SR2 and SR3, for models with $m_{\tilde{b}_1,\tilde{t}_1} = 600$ GeV, $m_{\tilde{\chi}_1^0} = 100$ GeV and $m_{\tilde{b}_1,\tilde{t}_1} = 500$ GeV, $m_{\tilde{\chi}_1^0} = 450$ GeV. The efficiencies of selections on the $H_{\mathrm{T},n}\,(n = 2, 3)$ variables used in SR2 and SR3 agree within a few percent for the sbottom and the corresponding stop pair sample with $\Delta m = 5$ GeV. With larger Δm, however, the difference in efficiency can be large. For example, with $m_{\tilde{t}} = 600$ GeV, $m_{\tilde{\chi}_1^0} = 100$ GeV and $\Delta m = 20$ GeV, the $H_{\mathrm{T},2} < 50$ GeV selection criterion is found to reduce the stop signal event yield by a factor of two compared to the corresponding sbottom scenario.

3 Results and interpretation

The results are interpreted in stop pair production scenarios in which the stop is assumed to decay via $\tilde{t}_1 \to b\tilde{\chi}_1^+$ with a 100% branching ratio. The mass difference between $\tilde{\chi}_1^+$ and $\tilde{\chi}_1^0$ is taken to be either 5 or 20 GeV. The signal samples are generated using `MADGRAPH` [20] interfaced to Pythia 6 [21], using the PDF set `CTEQ6L1` [22].

$(m_{\tilde{b}_1,\tilde{t}_1}, m_{\tilde{\chi}_1^0})$	sbottom		stop ($\Delta m = 5$ GeV)		stop ($\Delta m = 10$ GeV)		stop ($\Delta m = 20$ GeV)	
$= (500, 300)$ GeV	rel.	abs.	rel.	abs.	rel.	abs.	rel.	abs.
preselection	91%	91%	89%	89%	87%	87%	86%	86%
lepton veto	99%	90%	98%	87%	94%	82%	84%	72%
met>150	77%	70%	75%	66%	74%	60%	71%	51%
$\geq$2 jets	99%	69%	99%	65%	100%	60%	100%	51%
leading jet $p_T > 130$ GeV	85%	59%	83%	54%	84%	50%	82%	42%
second jet $p_T > 50$ GeV	91%	53%	92%	50%	91%	46%	90%	38%
third jet veto	48%	26%	47%	23%	48%	22%	45%	17%
$\Delta\phi(E_{\mathrm{T}}^{\mathrm{miss}}, j_{1,2,(3)}) > 0.4$	89%	23%	89%	21%	88%	19%	84%	14%
$E_{\mathrm{T}}^{\mathrm{miss}}/m_{\mathrm{eff}} > 0.25$	97%	22%	98%	20%	98%	19%	98%	14%
2 b-jets	35%	7.6%	33%	6.7%	34%	6.4%	33%	4.5%
$m_{CT} > 100$ GeV	94%	7.2%	93%	6.2%	94%	6.0%	96%	4.3%
$m_{CT} > 150$ GeV	85%	6.1%	84%	5.2%	81%	4.9%	79%	3.4%
$m_{CT} > 200$ GeV	66%	4.0%	62%	3.2%	58%	2.8%	56%	1.9%
$m_{CT} > 250$ GeV	38%	1.5%	37%	1.2%	30%	0.9%	29%	0.6%

Table 2: Selection efficiencies for a sbottom signal point with $m_{\tilde{b}_1} = 500$ GeV and $m_{\tilde{\chi}_1^0} = 300$ GeV (second and third columns), and three stop signal points with $m_{\tilde{t}_1} = 500$ GeV, $m_{\tilde{\chi}_1^0} = 300$ GeV for $\Delta m = 5$ GeV, 10 GeV and 20 GeV. The absolute selection efficiencies are computed with respect to the total number of simulated events, whereas relative efficiencies are computed with respect to the previous selection criterion. All numbers are extracted from samples whose total size is roughly 10000 events.

Experimental and theoretical uncertainties on the signal are included using the prescriptions discussed in Ref. [17].

The 95% confidence level (C.L.) exclusion limits obtained using the CL_s prescription [23] are shown in Fig. 3 for $\Delta m = 5$ GeV and in Fig. 4 for $\Delta m = 20$ GeV. The signal region with the best expected CL_s exclusion limit is used to derive the limit for each signal point.

If $m_{\tilde{\chi}_1^0} = 100$ GeV, stop quark masses up to 580 GeV are excluded at 95% C.L. for $\Delta m = 5$ GeV and 480 GeV for $\Delta m = 20$ GeV. Assuming $\Delta m = 5$ ($\Delta m = 20$) GeV, neutralino masses up to 300 (250) GeV are excluded for $m_{\tilde{t}_1} = 500(480)$ GeV.

4 Conclusions

The results of Ref. [17], based on 12.8 fb^{-1} of $\sqrt{s} = 8$ TeV pp collision data recorded by the ATLAS detector, are interpreted in scenarios where pair produced stops decay into a chargino and a bottom quark.

For $m_{\tilde{\chi}_1^0} = 100$ GeV, stop masses up to 580 GeV are excluded at 95% C.L. for $\Delta m = 5$ GeV and 480 GeV for $\Delta m = 20$ GeV. Assuming $\Delta m = 5$ GeV, neutralino masses up to 300 GeV are excluded for $m_{\tilde{t}_1} = 500$ GeV. Assuming $\Delta m = 20$ GeV, neutralino masses up to 250 GeV are excluded for $m_{\tilde{t}_1} = 480$ GeV.

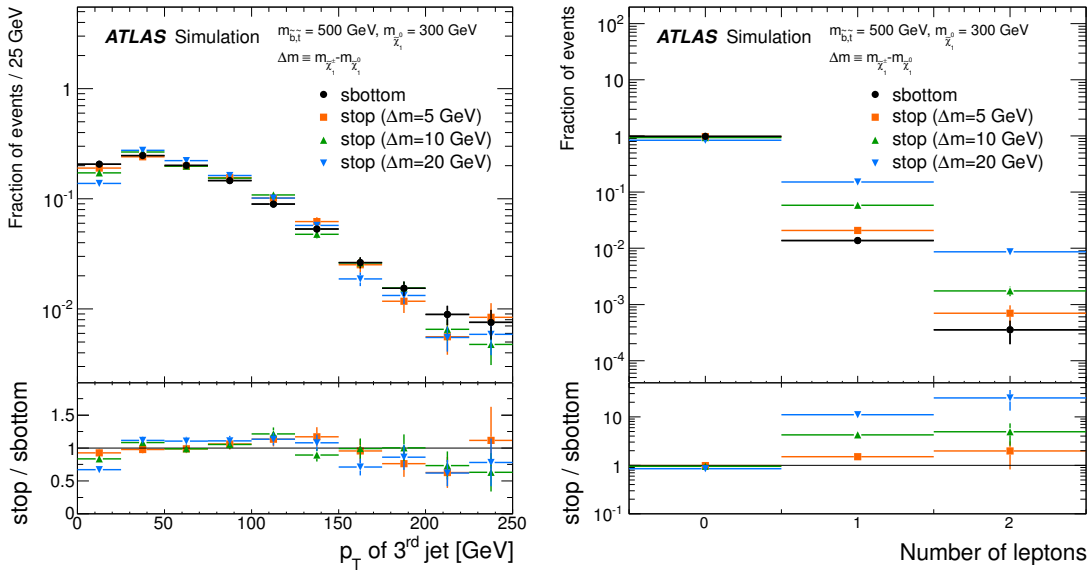

Figure 1: Comparison of distributions (normalised to unit area) for a sbottom signal point with $m_{\tilde{b}_1} = 500$ GeV and $m_{\tilde{\chi}_1^0} = 300$ GeV, and three stop signal points with $m_{\tilde{t}_1} = 500$ GeV, $m_{\tilde{\chi}_1^0} = 300$ GeV and $\Delta m = 5$ GeV, 10 GeV and 20 GeV. The p_T of the third highest momentum jet (left) and the number of electrons and muons with $p_T > 10$ GeV (right). The distribution of the p_T of the third highest momentum jet is produced after requiring all selection criteria up to and including the $p_T > 50$ GeV requirement on the second jet in Table 2. The distribution of the number of leptons is produced after the preselection. Only statistical uncertainties arising from the limited size of simulated samples are shown. The bottom panel in each plot shows the ratios of the histogram entries from the stop pair samples and the sbottom pair sample. The final bin in the histograms includes the overflow.

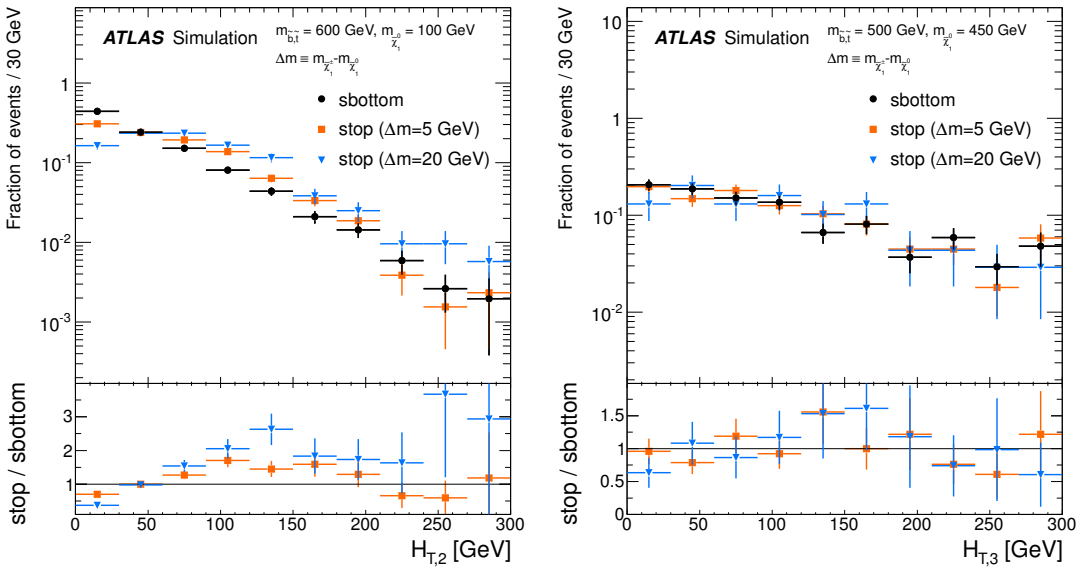

Figure 2: Comparison of distributions normalised to unit area for a sbottom pair signal point and two stop pair signal points with $\Delta m = 5$ and 20 GeV. Left: $H_{\mathrm{T},2}$ distribution for $m_{\tilde{b}_1} = m_{\tilde{t}_1} = 600$ GeV and $m_{\tilde{\chi}_1^0} = 100$ GeV. Right: $H_{\mathrm{T},3}$ distribution for $m_{\tilde{b}_1} = m_{\tilde{t}_1} = 500$ GeV and $m_{\tilde{\chi}_1^0} = 450$ GeV. The distribution of $H_{\mathrm{T},2}$ is produced after requiring all selection criteria up to and including the $p_T > 50$ GeV requirement on the second jet in Table 2. The distribution of $H_{\mathrm{T},3}$ is produced after requiring the leading jet to have $p_T > 130$ GeV and two additional jets with $p_T > 30$ GeV. Only statistical uncertainties arising from the limited size of simulated samples are shown. The bottom panel in each plot shows the ratios of the histogram entries from the stop pair samples to the sbottom pair sample. The final bin in the histograms includes the overflow.

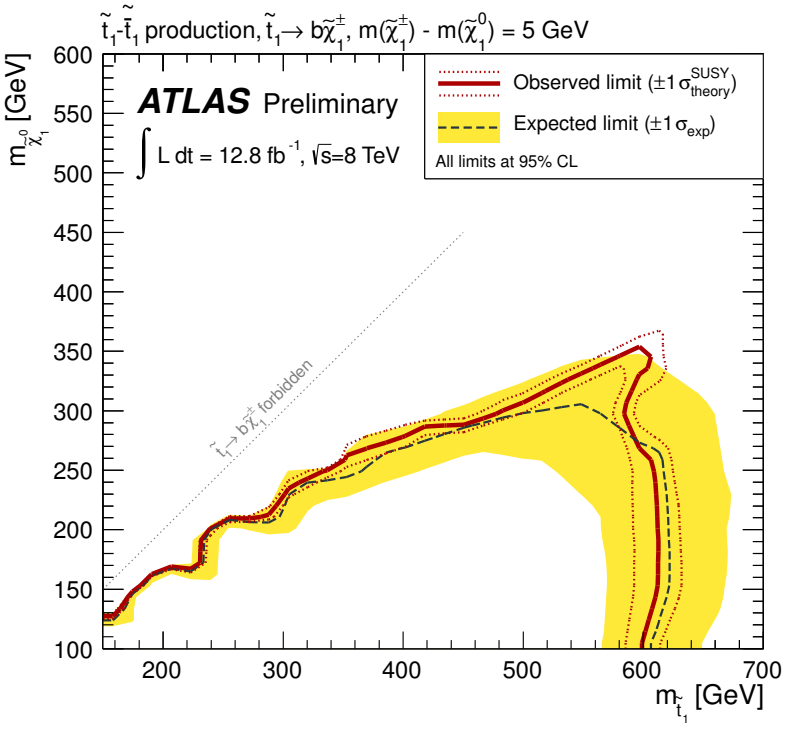

Figure 3: Expected and observed 95% C.L. exclusion limits in the $m_{\tilde{t}_1} - m_{\tilde{\chi}_1^0}$ plane for $\Delta m = 5$ GeV. The black, dashed line shows the expected limit if theoretical uncertainties on the signal are neglected. The yellow band shows the $\pm 1\sigma$ uncertainty on the expected limit. The red solid line shows the nominal observed limit, while the red dashed lines show its variation if theory uncertainties on the signal are taken into account.

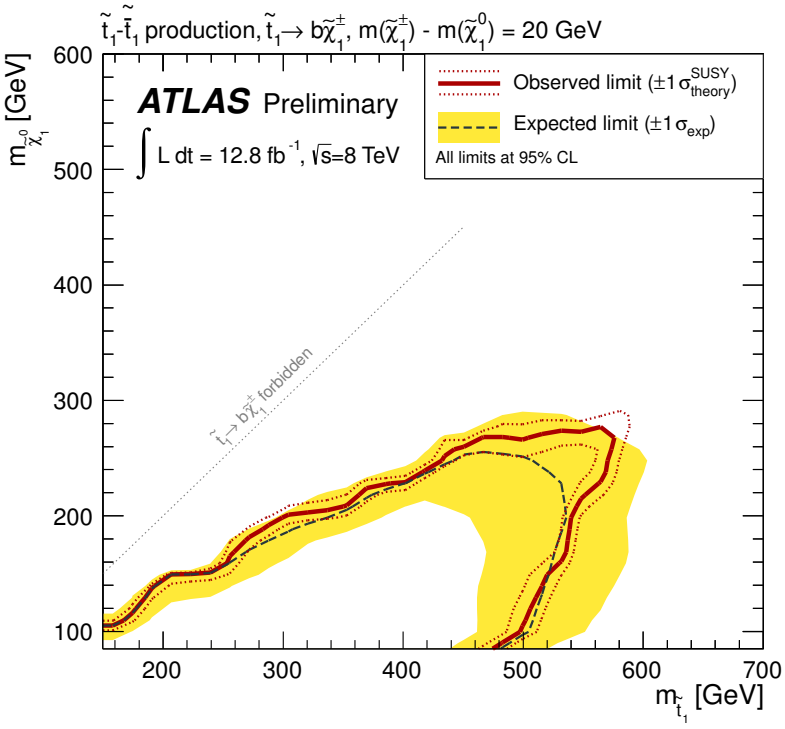

Figure 4: Expected and observed 95% C.L. exclusion limits in the $m_{\tilde{t}_1} - m_{\tilde{\chi}_1^0}$ plane for $\Delta m = 20$ GeV. The black, dashed line shows the expected limit if theoretical uncertainties on the signal are neglected. The yellow band shows the $\pm 1\sigma$ uncertainty on the expected limit. The red solid line shows the nominal observed limit, while the red dashed lines show its variation if theory uncertainties on the signal are taken into account.

A Auxiliary material

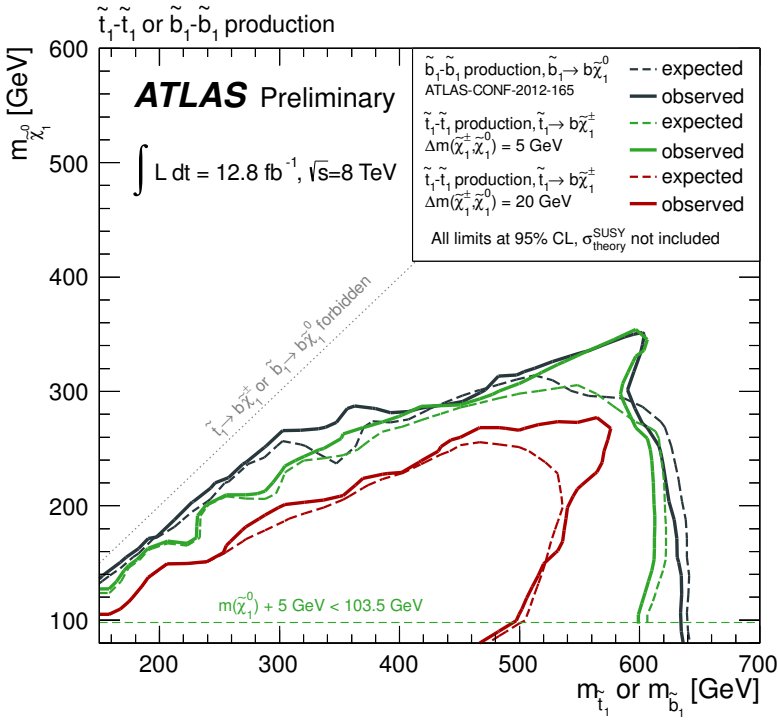

Figure 5: Expected and observed 95% C.L. exclusion limits on sbottom pair production in the $m_{\tilde{b}_1} - m_{\tilde{\chi}_1^0}$ plane, together with the expected and observed 95% C.L. exclusion limits for stop pair production in the $m_{\tilde{t}_1} - m_{\tilde{\chi}_1^0}$ plane for $\Delta m = 5$ GeV and 20 GeV. The theory uncertainty on the signal is not shown.

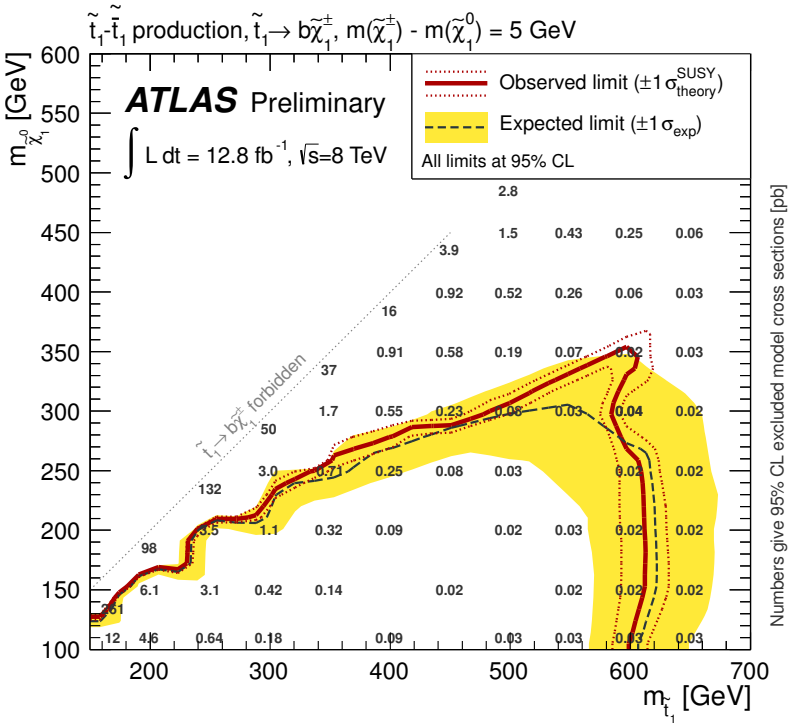

Figure 6: Expected and observed 95% C.L. exclusion limits in the $m_{\tilde{t}_1} - m_{\tilde{\chi}_1^0}$ plane for $\Delta m = 5$ GeV. The black, dashed line shows the expected limit if theory uncertainties on the signal are neglected. The yellow band shows the $\pm 1\sigma$ uncertainty on the expected limit. The red solid line shows the nominal observed limit, while the red dashed lines show its variation if theory uncertainties on the signal are taken into account. The overlaid numbers give the observed upper limit on the signal cross section, in pb. For clarity, numbers of the first row (column) have been shifted upwards (right) by 10 GeV.

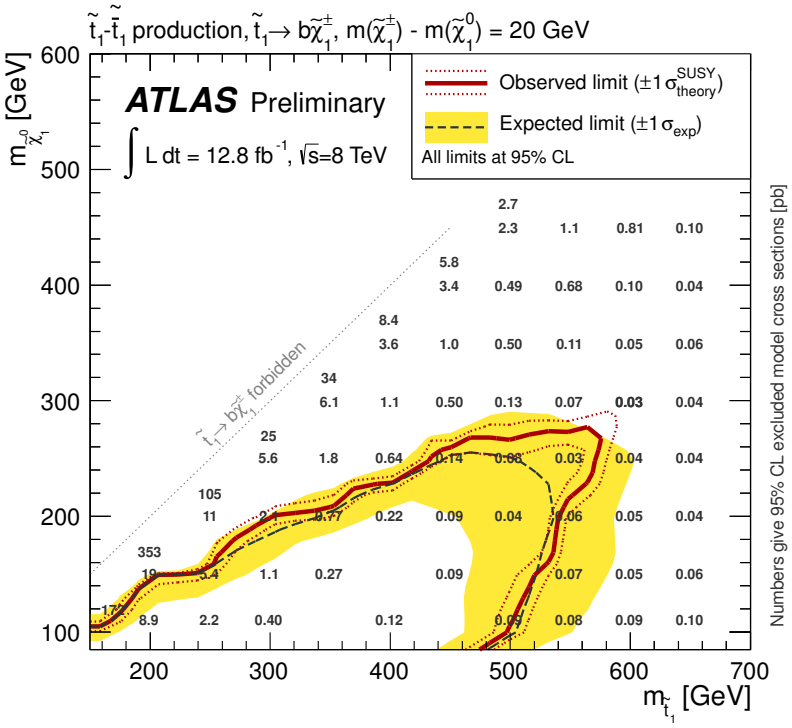

Figure 7: Expected and observed 95% C.L. exclusion limits in the $m_{\tilde{t}_1} - m_{\tilde{\chi}_1^0}$ plane for $\Delta m = 20$ GeV. The black, dashed line shows the expected limit if theory uncertainties on the signal are neglected. The yellow band shows the $\pm 1\sigma$ uncertainty on the expected limit. The red solid line shows the nominal observed limit, while the red dashed lines show its variation if theory uncertainties on the signal are taken into account. The overlaid numbers give the observed upper limit on the signal cross section, in pb. For clarity, the first column number has been shifted right by 10 GeV.

References

[1] H. Miyazawa, *Baryon Number Changing Currents*, Prog. Theor. Phys. **36 (6)** (1966) 1266–1276.

[2] P. Ramond, *Dual Theory for Free Fermions*, Phys. Rev. **D3** (1971) 2415–2418.

[3] Y. A. Gol'fand and E. P. Likhtman, *Extension of the Algebra of Poincare Group Generators and Violation of p Invariance*, JETP Lett. **13** (1971) 323–326. [Pisma Zh.Eksp.Teor.Fiz.13:452-455,1971].

[4] A. Neveu and J. H. Schwarz, *Factorizable dual model of pions*, Nucl. Phys. **B31** (1971) 86–112.

[5] A. Neveu and J. H. Schwarz, *Quark Model of Dual Pions*, Phys. Rev. **D4** (1971) 1109–1111.

[6] J. Gervais and B. Sakita, *Field theory interpretation of supergauges in dual models*, Nucl. Phys. **B34** (1971) 632–639.

[7] D. V. Volkov and V. P. Akulov, *Is the Neutrino a Goldstone Particle?*, Phys. Lett. **B46** (1973) 109–110.

[8] J. Wess and B. Zumino, *A Lagrangian Model Invariant Under Supergauge Transformations*, Phys. Lett. **B49** (1974) 52.

[9] J. Wess and B. Zumino, *Supergauge Transformations in Four-Dimensions*, Nucl. Phys. **B70** (1974) 39–50.

[10] S. Weinberg, *Implications of Dynamical Symmetry Breaking*, Phys. Rev. **D13** (1976) 974–996.

[11] E. Gildener, *Gauge Symmetry Hierarchies*, Phys. Rev. **D14** (1976) 1667.

[12] S. Weinberg, *Implications of Dynamical Symmetry Breaking: An Addendum*, Phys. Rev. **D19** (1979) 1277–1280.

[13] L. Susskind, *Dynamics of Spontaneous Symmetry Breaking in the Weinberg- Salam Theory*, Phys. Rev. **D20** (1979) 2619–2625.

[14] R. Barbieri and G. Giudice, *Upper Bounds on Supersymmetric Particle Masses*, Nucl.Phys. **B306** (1988) 63.

[15] B. de Carlos and J. Casas, *One loop analysis of the electroweak breaking in supersymmetric models and the fine tuning problem*, Phys.Lett. **B309** (1993) 320–328, `arXiv:hep-ph/9303291 [hep-ph]`.

[16] M. Papucci, J. T. Ruderman, and A. Weiler, *Natural SUSY Endures*, JHEP **1209** (2012) 035, `arXiv:1110.6926 [hep-ph]`.

[17] ATLAS Collaboration, *Search for scalar bottom pair production in final states with missing transverse momentum and two b-jets in pp collisions at* $\sqrt{s} = 7$ *TeV with the ATLAS Detector*, ATLAS-CONF-2012-165 (2012) , `https://cds.cern.ch/record/1497668`.

[18] LEP SUSY Working Group (ALEPH, DELPHI, L3, OPAL), Notes LEPSUSYWG/01-03.1 and 04-01.1, http://lepsusy.web.cern.ch/lepsusy/Welcome.html.

[19] W. Beenakker, S. Brensing, M. Kramer, A. Kulesza, E. Laenen, and I. Niessen, *Supersymmetric top and bottom squark production at hadron colliders*, JHEP **1008** (2010) 098, arXiv:1006.4771 [hep-ph].

[20] M. Bahr, S. Gieseke, M. Gigg, D. Grellscheid, K. Hamilton, et al., *Herwig++ Physics and Manual*, Eur. Phys. J. **C58** (2008) 639–707, arXiv:0803.0883 [hep-ph].

[21] T. Sjöstrand, S. Mrenna, and P. Skands, *PYTHIA 6.4 physics and manual*, JHEP **0605** (2006) 026.

[22] J. Pumplin et al., *New generation of parton distributions with uncertainties from global QCD analysis*, JHEP **0207** (2002) 012.

[23] G. Cowan, K. Cranmer, E. Gross, and O. Vitells, *Asymptotic formulae for likelihood-based tests of new physics*, Eur. Phys. J. **C71** (2011) 1–19.